Commun Nonlinear Sci Numer Simulat 44 (2017) 204–219

Contents lists available at ScienceDirect

Commun Nonlinear Sci Numer Simulat

journal homepage: www.elsevier.com/locate/cnsns

Research paper

Comparison between two meshless methods based on collocation technique for the numerical solution of four-species tumor growth model

Mehdi Dehghan*, Vahid Mohammadi

Department of Applied Mathematics, Faculty of Mathematics and Computer Sciences, Amirkabir University of Technology, No. 424, Hafez Ave., 15914, Tehran, Iran

ARTICLE INFO

Article history:
Received 16 June 2015
Revised 8 June 2016
Accepted 22 July 2016
Available online 25 July 2016

MSC:
65N35

Keywords:
Four-species tumor-growth model
Two and three-dimensional equations
Meshless collocation technique
Explicit time integration
Mathematical biology

ABSTRACT

As is said in [27], the tumor-growth model is the incorporation of nutrient within the mixture as opposed to being modeled with an auxiliary reaction-diffusion equation. The formulation involves systems of highly nonlinear partial differential equations of surface effects through diffuse-interface models [27]. Simulations of this practical model using numerical methods can be applied for evaluating it. The present paper investigates the solution of the tumor growth model with meshless techniques. Meshless methods are applied based on the collocation technique which employ multiquadrics (MQ) radial basis function (RBFs) and generalized moving least squares (GMLS) procedures. The main advantages of these choices come back to the natural behavior of meshless approaches. As well as, a method based on meshless approach can be applied easily for finding the solution of partial differential equations in high-dimension using any distributions of points on regular and irregular domains. The present paper involves a time-dependent system of partial differential equations that describes four-species tumor growth model. To overcome the time variable, two procedures will be used. One of them is a semi-implicit finite difference method based on Crank–Nicolson scheme and another one is based on explicit Runge–Kutta time integration. The first case gives a linear system of algebraic equations which will be solved at each time-step. The second case will be efficient but conditionally stable. The obtained numerical results are reported to confirm the ability of these techniques for solving the two and three-dimensional tumor-growth equations.

* Corresponding author.
E-mail addresses: mdehghan@aut.ac.ir, mdehghan.aut@gmail.com (M. Dehghan), v.mohammadi@aut.ac.ir (V. Mohammadi).

http://dx.doi.org/10.1016/j.cnsns.2016.07.024
1007-5704/

1. Introduction

1.1. Mathematical model

The split of the fourth-order differential equations into two second-order differential equations for four-species tumor growth model is considered as follows [27]:

$$\begin{cases} u_t = \nabla.(M_u \nabla \mu_u) + \gamma_u, \\ \mu_u = f'(u) - \varepsilon^2 \Delta u + D_u \chi(u,n), \\ n_t = \nabla.(M_n \nabla \mu_n) - \gamma_u, \\ \mu_n = D_n \chi(u,n) + \dfrac{n}{\delta}, \end{cases} \tag{1.1}$$

where M_u is variable or constant mobility. $f(u)$ denotes the free-energy density function. μ_u and μ_n also are the chemical potentials with respect to u and n, respectively. γ is a constant parameter.

The boundary and initial conditions for this practical model are as follows [27]:

$$\begin{aligned} &\frac{\partial u}{\partial \vec{\mathbf{n}}} = \frac{\partial \mu_u}{\partial \vec{\mathbf{n}}} = \frac{\partial n}{\partial \vec{\mathbf{n}}} = \frac{\partial \mu_n}{\partial \vec{\mathbf{n}}} = 0, \quad && \text{on} \partial\Omega, \\ &u(\mathbf{x},\mathbf{0}) = \mathbf{u_0}(\mathbf{x}), && \mu_u(\mathbf{x},\mathbf{0}) = \mu_{\mathbf{u0}}(\mathbf{x}), \\ &n(\mathbf{x},\mathbf{0}) = \mathbf{n_0}(\mathbf{x}), && \mu_n(\mathbf{x},\mathbf{0}) = \mu_{\mathbf{n0}}(\mathbf{x}), \ \mathbf{x} \in \boldsymbol{\Omega} \subset \mathbb{R}^{\mathbf{d}}, \end{aligned}$$

where d usually is equal to 2 and 3. In Eq. (1.1), $\vec{\mathbf{n}}$ is a unit normal vector. The nonlinear free-energy density function i.e. $f(u)$ can be considered as follows [63]:

$$f(u) = \begin{cases} (u+1)^2, & u < -1, \\ \dfrac{1}{4}(u^2-1)^2, & -1 \le u \le 1, \\ (u-1)^2, & u > 1. \end{cases} \tag{1.2}$$

Moreover, it can be defined in the following formula [27]:

$$f(u) = \Gamma u^2 (1-u)^2, \quad u \in [0,1], \tag{1.3}$$

where Γ is a constant parameter. Also we have

$$\chi(u,n) = -X_0 u\, n, \quad \gamma_u = P_0 u\, n + \delta P_0 u (D_n \chi(u,n) - \mu_u),$$

in which δ and X_0 are positive constants and P_0 is proliferation rate [27]. u denotes the tumor cell volume fraction and n shows the nutrient-rich extracellular water volume fraction [27]. The total energy is defined as follows [27]:

$$\int_\Omega \left(f(u) + \frac{\varepsilon^2}{2} |\nabla u|^2 + \chi(u,n) + \frac{1}{2\delta^2} n^2 \right) d\Omega,$$

where ϵ^2 is the diffusivity parameter for the surface energy term, $\chi(u, n)$ is the chemotaxis energy, and $\delta > 0$ is a small parameter governing the relative strength of the interaction among the cell and nutrient species [27]. The property of mass conservation remains as follows:

$$\int_\Omega (u(\mathbf{x},t) + n(\mathbf{x},t))\, d\Omega = \int_\Omega (u(\mathbf{x},0) + n(\mathbf{x},0))\, d\Omega.$$

1.2. Deriving four-species mixture

The description of components of a four-species model is: the tumor cell concentration and the healthy cell concentration along with two species identified with extra-cellular water [27]. The mixture is composed by the following four species [27]:

- $u :=$ tumor cell volume fraction,
- $h :=$ healthy cell volume fraction,
- $n :=$ nutrient-rich extracellular water volume fraction,
- $w :=$ nutrient-poor extracellular water volume fraction.

An example of mixture is shown in Fig. 1. When $u + h + n + w = 1$, the mixture is assumed to be saturated everywhere. Additional constraints are applied, the total concentration of cells remains constant throughout the domain, that means $u + h = C$ everywhere. Thus, $n + w = 1 - C$, everywhere. According to $u + h + n + w = 1$, the constant C can be rescaled such that u, h, n and w be admissible between 0 and 1.

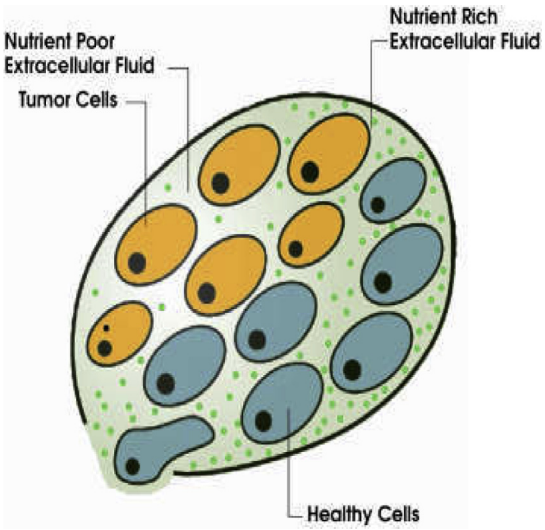

Fig. 1. Four-species model: illustration of the four-species mixture [27].

The equations for the balance of mass for each constituent are as follows [44]:

$$\begin{cases} u_t = \nabla.(M_u \nabla \mu_u) + \gamma_u, \\ h_t = \nabla.(M_h \nabla \mu_h) + \gamma_h, \\ n_t = \nabla.(M_n \nabla \mu_n) + \gamma_n, \\ w_t = \nabla.(M_w \nabla \mu_w) + \gamma_w. \end{cases}$$

Note that, the chemical potentials i.e. $(\mu_u, \mu_h, \mu_n, \mu_w)$ are obtained from the Gateaux derivative of free-energy function [27]. Constraints on the constitutive relations which are derived in [44], must be satisfied as follows [27]:

$$\begin{cases} \gamma_u + \gamma_h + \nabla.(M_u \nabla \mu_u) + \nabla.(M_h \nabla \mu_h) = 0, \\ \gamma_n + \gamma_w + \nabla.(M_n \nabla \mu_n) + \nabla.(M_w \nabla \mu_w) = 0. \end{cases} \tag{1.4}$$

Moreover, it must be satisfied

$$\mu_u \gamma_u + \mu_h \gamma_h + \mu_n \gamma_n + \mu_w \gamma_w \leq 0. \tag{1.5}$$

Considering these assumptions and the free function i.e. $f(u)$ and the energy functionals i.e. E gives the following chemical potentials [27]:

$$\begin{cases} \mu_u = f'(u) - \varepsilon^2 \Delta u + D_u \chi(u, n), \\ \mu_h = f'(C-h) - \varepsilon^2 \Delta (C-h) - D_u \chi(C-h, n), \\ \mu_n = D_n \chi(u, n) + \dfrac{n}{\delta}, \\ \mu_w = -D_n \chi(u, (1-C) - w) - \dfrac{((1-C) - w)}{\delta}. \end{cases}$$

Summing each side of the above equations yields

$$\mu_u + \mu_h + \mu_n + \mu_w = 0.$$

With this, we have $\gamma_u + \gamma_h = 0$ and $\gamma_n + \gamma_w = 0$. On the other hand, $u_t + h_t = n_t + w_t = 0$. Thus, the governing equations for u and n can be written explicitly

$$\begin{cases} u_t = \nabla.(M_u \nabla (f'(u) - \varepsilon^2 \Delta u + D_u \chi(u, n))) + \gamma_u, \\ n_t = \nabla.\left(M_n \nabla \left(D_n \chi(u, n) + \dfrac{n}{\delta}\right)\right) + \gamma_n, \end{cases}$$

with constraints (1.4) and (1.5).

It should be noted that, the continuum theory of mixtures is considered for introducing the four-species mixture tumor growth model [27,57]. For more details, the interested readers refer to [27,57] and references therein.

1.3. A brief explanation about the tumor growth model

As mentioned in [27], the computational models of tumor growth are gradually becoming an accepted mode of investigating the behavior and the response of tumors to various environment conditions and possible treatments [27]. The idea that such a model could predict, even qualitatively, the emergence, growth, or decline of tumors in living tissue is enormously intriguing [63]. The tumor growth is considered for a multiscale modeling phenomena, early experiments were only able to capture and interpret events happening on a single macroscale. There were many advances in experimental techniques and methods developed in 1980 such as polymerase chain reaction [7], many discoveries have been made concerning mechanisms now known to be critical to tumor growth, including the six hallmarks of cancer, such as angiogenesis, cell movement, and cell mutations [28]. In recent years the number of mathematical models of tumor growth has dramatically increased along with the general level of complexity. For example, in 2004, Araujo and McElwain [2], and several surveys of models have also appeared in more recent years, that is, those compiled in Wodarz and Komarova [62], Bellomo et al. [10], Preziosi [48], Lowengrub et al. [37], and many others [8,9,14,24,25,45,49,61]. The model of tumor growth can be divided to the three categories as follows [27]:

1. Discrete models.
2. Cellular automata models.
3. Continuum models.

The continuum theory of mixtures provides a mathematical framework for incorporating multiple phases within a single model [27]. The framework for the continuum theory of mixtures was introduced in 1960 and 1976 by Truesdell and Toupin [56] and Bowen [13], respectively. By the mid-1990s, it was regarded as a fairly mature theory for describing non-biologically growing media. In 1998, the first model was introduced [46] exploring in one dimension, the possible formation of a necrotic core due to stress within the tumor in the context of two phases: tumor cells, assumed inviscid, and extracellular water. Shortly afterward, this model was extended to three dimensions and included surface tension [47]. A different approach was used by Breward et al. [12], who assumed the existence of an inviscid aqueous phase but allowed the viscosity of the tumor cells to vary as a function of their level of differentiation, higher differentiation corresponding to higher viscosity. This approach was an attempt to simulate the cellûcell interactions that form between cells. Two other models were proposed by Preziosi and Farina [48] and Araujo and McElwain [1], in which a solid matrix was considered to be presented among the other two phases, in the spirit of porous media. These models have been extended to include the host tissue as a third phase [3] and to begin considering multiscale adhesion effects resulting from surface molecules attaching to the extracellular matrix [16]. Other models include blood vessels [12], interstitial fluid pressure aspects of the tumor tissue especially in regard to vascular collapse [1,15,51,54]. These models influence by many experiments showing that pressure and stress values were different in tumorous and healthy tissue and that vascular collapse was non-uniformly present throughout the tumor, implying the presence of residual stresses. A four-phase model by Wise et al. is introduced [57,58]. The introduced model consists of tumor live cells, tumor dead cells, host cells, and an extracellular fluid, in contrast to the other mixture models under the influence of a convective velocity. Also, a group of this model has been developed as a two-phase diffuse-interface model of tumor growth including a chemotaxis term in the free-energy [17].

1.4. The literature review and the current work

In recent years, there are some numerical methods for obtaining the numerical solution of the tumor growth model. Some of them are: second-order time-accurate methods [22], an implicit Taylor approximation of the secant form also results in an unconditionally-stable (and nonlinear) scheme [35], an efficient numerical method for analyzing spinodal decomposition presented by the Cahn-Hilliard equation [59], the extensions of the secant-based schemes to systems with more than two phases [11]. An alternative to the secant form is applied in [26]. Their unconditionally-stable nonlinear scheme can be interpreted as a standard Crank–Nicolson scheme with additional stabilization. Another seemingly natural alternative would be to search for second-order splitting-based schemes. This idea has been pursued by Hu, Wise, Wang and Lowengrub [29] and by Shen, Wang, Wang and Wise [53]. A Galerkin finite element method has been applied for four-species tumor growth model [27]. In [63], the authors provided the stabilized second-order convex splitting schemes. With our best of knowledge, the current paper is the first research work on employing the meshless methods for finding the numerical solution of the present model. There has been a growing interest for applying the meshless techniques to obtain the numerical solution of partial differential equations in recent years.

The method of radial basis functions (RBFs) is well-known as a suitable meshless method for the solution of partial differential equations of various types in the literature works. A direct collocation method based on RBFs namely Kansa's approach. The main advantage of this method is: easy implementation for high-dimension problems in comparison with the other meshless techniques. Moreover, RBFs method performs very well in interpolating highly irregular scattered data compared to many interpolating methods. RBFs have a constant parameter which is called shape parameter. It plays a vitally significant role for finding solution of interpolation and partial differential equations. Another meshless technique is named moving least squares approximation (MLS) and it solves a locally weighted least squares problem for each point $\mathbf{x}$ (in the domain of the problem) [60]. Recently, Mirzaei et. al [41] introduced the generalized moving least squares method

(GMLS) which can be implemented easily in comparison with the classical version i.e. MLS approximation. In Fact, the GMLS approximation is based on direct approximation [41]. The other meshless techniques can be found in [4,5,6,20,21,30,38,55].

1.5. The main aim of this paper

The remainder of this paper is as follows:
Section 2 explains on the two numerical meshless methods based on collocation technique which will be applied for solving the present model. Next section introduces the use of Runge–Kutta technique for overcoming the time variable and it will be combined with efficient MLS method i.e. GMLS procedure. The numerical simulations will be presented in Section 4. Section 5 gives some remarks about the applied numerical meshless methods.

2. Methods discussion and mathematical formulations

In this section, two meshless techniques will be applied for solving tumor growth model. Before using these techniques, first, the semi-implicit method based on Crank–Nicolson scheme for time discretization will be used. To do it, the time interval $[0, T]$ is divided to M sub-intervals such that $\tau(=\Delta t)=\frac{T}{M}$ $t^k = k\tau,\ k=0,1,2,\ldots,M-1$. With this, Eq. (1.1) can be discritized with respect to time as follows:

$$\begin{cases} u^{k+1}-\dfrac{\tau}{2}(\Delta\mu_u)^{k+1}=u^k+\dfrac{\tau}{2}(\Delta\mu_u)^k+\tau(\gamma_u)^k,\\ \phi_u(u^{k+1})+\varepsilon^2\dfrac{\Delta u^{k+1}}{2}+\dfrac{(\mu_u)^{k+1}}{2}+\phi_n(n^{k+1})=\phi_u(u^k)-\varepsilon^2\dfrac{\Delta u^{k+1}}{2}-\dfrac{(\mu_u)^{k+1}}{2}+\phi_n(n^k),\\ n^{k+1}-\dfrac{\tau}{2}(\Delta\mu_n)^{k+1}=n^k+\dfrac{\tau}{2}(\Delta\mu_n)^k-\tau(\gamma_u)^k,\\ \nu_u(u^{k+1})+\dfrac{(\mu_n)^{k+1}}{2}-\dfrac{n^{k+1}}{2\delta}=\nu_u(u^k)-\dfrac{(\mu_n)^k}{2}+\dfrac{n^k}{2\delta},\ k=0,1,2,\ldots,M-1. \end{cases} \tag{2.1}$$

2.1. Implementation of the GMLS technique on tumor growth model with constant mobility

For the first time, Lancaster and Salkauskas introduced the moving least squares method (MLS) in 1981 [36]. One main advantage of this technique is to solve a locally weighted least squares problem for every point $\mathbf{x}$ [60]. As can be observed in the literature about MLS approximation, in this method, we need the derivatives of the weight functions. This yields high computational cost by increasing the collocation points. Recently, a new approach based on MLS approximation is developed by Mirzaei et al. [41] namely generalized moving least squares method (GMLS). In their new technique, the linear functionals act only on polynomial basis functions without any detour via classical MLS shape functions. In fact, this is a direct approximation [40,52]. Now, we apply this technique for solving our model in this paper.

Let $\Omega\subset\mathbb{R}^d$ be a nonempty and bounded set. Suppose that N scattered points $X=\{\mathbf{x}_1,\mathbf{x}_2,\ldots,\mathbf{x}_N\}\subset\Omega$ are given. Moreover, $\{p_1,p_2,\ldots,p_Q\}$ be a basis for the space $\mathbb{P}_m^d$ (the space of d-variable polynomials of degree at most m of dimension $Q=\binom{m+d}{d}$).

MLS approximation [36,39,41,42,60] of unknown function $u(\mathbf{x})$ which is defined on the region Ω, can be written in the following form:

$$u(\mathbf{x})\approx\overline{u(\mathbf{x})}=\sum_{j=1}^{N}a_j(\mathbf{x})u(\mathbf{x}_j),\quad \mathbf{x}\in\Omega, \tag{2.2}$$

in which $a_j(\mathbf{x})$ are the shape functions of MLS. Note that, $a_j(\mathbf{x})$ constructed such that $\bar{u}$ be the best approximation of u in polynomial subspace $\mathbb{P}_m^d$ with respect to a weighted discrete moving l_2-norm. The weight function w is assumed to be $w:\Omega\times\Omega\mapsto\mathbb{R}$ and governs the influence of the data points. This function is defined as follows:

$$w(\mathbf{x},\mathbf{x}_j)=\begin{cases}\varphi\left(\dfrac{||\mathbf{x}-\mathbf{x}_j||_2}{\delta}\right) & ||\mathbf{x}-\mathbf{x}_j||_2\le\delta,\\ 0, & ||\mathbf{x}-\mathbf{x}_j||_2>\delta.\end{cases}$$

where δ is the radius of support domain. The weight function is as the compactly supported function on [0, 1]. Also we define

$$P=p(\mathbf{x})=(p_k(\mathbf{x}_j))\in\mathbb{R}^{N\times Q},\quad W=W(\mathbf{x})=diag\{w(\mathbf{x}_j,\mathbf{x})\}\in\mathbb{R}^{N\times N}.$$

By a simple calculation, the shape functions of MLS can be obtained in the following form [36,39–42,60]:

$$a(\mathbf{x}):=[a_1(\mathbf{x})\ a_2(\mathbf{x})\ldots a_N(\mathbf{x})]^T=\mathbf{p}(\mathbf{x})(P^TWP)^{-1}P^TW,$$

in which $\mathbf{p} = [p_1, p_2, \ldots, p_Q]^T$. For well-conditioning the MLS approximation at sample $\mathbf{x}$, the matrix $A(\mathbf{x}) = P^T W P$ must be invertible. For this purpose, if $X_{\mathbf{x}} = \{\mathbf{x} : ||\mathbf{x} - \mathbf{x}_j|| \leq \delta\}$ is $\mathbb{P}_m^d$-unisolvent then the matrix $A(\mathbf{x})$ is positive definite and thus is invertible [36,39–42,60]. The derivatives of u are approximated by derivative $\bar{u}$ with respect to the multi-index $\alpha \in \mathbb{N}_0^d$, $|\alpha| = \alpha_1 + \alpha_2 + \ldots + \alpha_d$ as follows [40–42]:

$$D^\alpha u(\mathbf{x}) \approx D^\alpha \overline{u(\mathbf{x})} = \sum_{j=1}^{N} D^\alpha a_j(\mathbf{x}) u(\mathbf{x}_j), \quad \mathbf{x} \in \Omega. \tag{2.3}$$

GMLS approximation can be defined as follows [40–42]:

$$\lambda u(\mathbf{x}) \approx \lambda \overline{u(\mathbf{x})} = \sum_{j=1}^{N} a_j(\lambda) u(\mathbf{x}_j), \quad \mathbf{x} \in \Omega, \tag{2.4}$$

in which λ is a linear functional [40–42]. Also, $a_j(\lambda)$ are shape functions with respect to the λ. In fact, we have [40–42]:

$$a(\lambda) := [a_1(\lambda)\ a_2(\lambda) \ldots a_N(\lambda)]^T = \lambda(\mathbf{p})(P^T W P)^{-1} P^T W,$$

where $\lambda(\mathbf{p}) = [\lambda(p_1), \lambda(p_2), \ldots, \lambda(p_Q)]^T$. It should be noted that, the main idea behind the method of GMLS approximation is: λ acts only on polynomial basis functions. This type of approximation reduces the computational cost in comparison with MLS procedure [40–42]. For more details, the interest readers refer to [40–42]. If in (2.4) $\lambda := D^\alpha u$, then we have:

$$D^\alpha u(\mathbf{x}) \approx D^\alpha \overline{u(\mathbf{x})} = \sum_{j=1}^{N} a_{j,\alpha}(\mathbf{x}) u(\mathbf{x}_j), \quad \mathbf{x} \in \Omega, \tag{2.5}$$

in which

$$a_\alpha(\mathbf{x}) = D^\alpha(\mathbf{p})(P^T W P)^{-1} P^T W.$$

Error bounds for the GMLS approximation are developed in [40,41]:

Now to implement the GMLS approximation, we consider N_i points in each support domain Ω_i. According to Eq. (2.1) at interior points $\mathbf{x}_j$, we obtain [40–42]:

$$\begin{cases} u_i^{k+1} - \dfrac{\tau}{2}(\Delta\mu_u)_i^{k+1} = u_i^k + \dfrac{\tau}{2}(\Delta\mu_u)_i^k + \tau(\gamma_u)_i^k, \\ \phi_u(u_i^{k+1}) + \varepsilon^2 \dfrac{\Delta u_i^{k+1}}{2} + \dfrac{(\mu_u)_i^{k+1}}{2} + \phi_n(n_i^{k+1}) = \phi_u(u_i^k) - \varepsilon^2 \dfrac{\Delta u_i^{k+1}}{2} - \dfrac{(\mu_u)_i^{k+1}}{2} + \phi_n(n_i^k), \\ n_i^{k+1} - \dfrac{\tau}{2}(\Delta\mu_n)_i^{k+1} = n_i^k + \dfrac{\tau}{2}(\Delta\mu_n)_i^k - \tau(\gamma_u)_i^k, \\ v_u(u_i^{k+1}) + \dfrac{(\mu_n)_i^{k+1}}{2} - \dfrac{n_i^{k+1}}{2\delta} = v_u(u_i^k) - \dfrac{(\mu_n)_i^k}{2} + \dfrac{n_i^k}{2\delta}, \quad k = 0, 1, 2, \ldots, M-1. \end{cases} \tag{2.6}$$

For each boundary point in the support domain Ω_i, we have

$$\frac{\partial u_i^{k+1}}{\partial \vec{\mathbf{n}}} = \frac{\partial(\mu_n)_i^{k+1}}{\partial \vec{\mathbf{n}}} = \frac{\partial(n)_i^{k+1}}{\partial \vec{\mathbf{n}}} = \frac{\partial(\mu_u)_i^{k+1}}{\partial \vec{\mathbf{n}}} = 0, \quad k = 0, 1, 2, \ldots, M-1. \tag{2.7}$$

Eqs. (2.6) and (2.7) yield the following linear system of algebraic equations:

$$A\Lambda^{k+1} = B\Lambda^k + \mathbf{b}^k, \ k = 0, 1, 2, \ldots, M-1. \tag{2.8}$$

Remark 2.1. The polynomial basis which are applied in two and three dimensions can be considered as follows:

$\mathbf{p} = [1, x, y, x^2, xy, y^2]^T$, **Two-dimensional case**,

$\mathbf{p} = [1, x, y, z, x^2, xy, xz, y^2, yz, z^2]^T$, **Three-dimensional case**.

Remark 2.2. The GMLS approximation is implemented in a more stable fashion [43]. For this purpose, if we consider a shifted and scaled polynomial basis function, then we have [43]:

$$\left\{ \frac{(x - x_i)^\alpha}{h_{X,\Omega}} \right\}_{0 \leq |\alpha| \leq m},$$

in which x_i is fixed and depends on the evaluation point. Also $h_{X,\Omega}$ is fill distance and is defined as follows [60]:

$$h_{X,\Omega} = \mathbf{sup}_{\mathbf{x} \in \Omega} \mathbf{min}_{\mathbf{x}_j \in X} ||\mathbf{x} - \mathbf{x}_j||_2.$$

Remark 2.3. The Wendland's function will be applied as weight function in the following definition [60]:

$$w(r_i) = w(||\mathbf{x} - \mathbf{x}_i||_2) = (1 - r)_+^4 (4r + 1) = \begin{cases} (1 - r)^4 (4r + 1), & 0 \leq r \leq 1, \\ 0, & r > 1, \end{cases}$$

in which $w \in C^2([0, \infty))$.

2.2. RBFs Interpolation based on Kansa's approach for solving tumor growth model with constant mobility

The method of RBFs based on collocation points is considered here. We approximate $u(\mathbf{x}, t^k)$, $\mu_u(\mathbf{x}, t^k)$, $n(\mathbf{x}, t^k)$ and $\mu_n(\mathbf{x}, t^k)$ with N collocation points $X = \{\mathbf{x}_1, \mathbf{x}_2, \ldots, \mathbf{x}_N\} \subset \Omega \subset \mathbb{R}^2$, in which $N = N_b + N_I$, N_b and N_I denote the number of boundary and interior points, respectively. These approximations can be written as follows [31–34]:

$$\begin{cases} u(\mathbf{x}, t^k) \approx \sum_{j=1}^{N} \alpha_j^k \varphi_j(\mathbf{x}), & \mu_u(\mathbf{x}, t^k) \approx \sum_{j=1}^{N} \beta_j^k \varphi_j(\mathbf{x}), \\ n(\mathbf{x}, t^k) \approx \sum_{j=1}^{N} \gamma_j^k \varphi_j(\mathbf{x}) & \mu_n(\mathbf{x}, t^k) \approx \sum_{j=1}^{N} \lambda_j^k \varphi_j(\mathbf{x}). \end{cases} \tag{2.9}$$

Now, we put Eq. (2.9) into the time discretization Eq. (2.1). Thus at interior points ($i = 1, 2, \ldots, N_I$) we have [18,19]

$$\begin{cases} \sum_{j=1}^{N} \alpha_j^{k+1} \varphi_j(\mathbf{x}_i) - \frac{\tau}{2} \sum_{j=1}^{N} \beta_j^{k+1} \Delta\varphi_j(\mathbf{x}_i) = \sum_{j=1}^{N} \alpha_j^k \varphi_j(\mathbf{x}_i) + \frac{\tau}{2} \sum_{j=1}^{N} \beta_j^k \Delta\varphi_j(\mathbf{x}_i) + \tau (\gamma_u)^k{}_i, \\ \phi_u\left(\sum_{j=1}^{N} \alpha_j^{k+1} \varphi_j(\mathbf{x}_i)\right) + \varepsilon^2 \frac{\sum_{j=1}^{N} \alpha_j^{k+1} \Delta\varphi_j(\mathbf{x}_i)}{2} + \frac{\sum_{j=1}^{N} \beta_j^{k+1} \Delta\varphi_j(\mathbf{x}_i)}{2} + \phi_n\left(\sum_{j=1}^{N} \gamma_j^{k+1} \varphi_j(\mathbf{x}_i)\right) \\ \quad = \phi_u\left(\sum_{j=1}^{N} \alpha_j^k \varphi_j(\mathbf{x}_i)\right) - \varepsilon^2 \frac{\sum_{j=1}^{N} \alpha_j^k \Delta\varphi_j(\mathbf{x}_i)}{2} - \frac{\sum_{j=1}^{N} \beta_j^k \Delta\varphi_j(\mathbf{x}_i)}{2} + \phi_n\left(\sum_{j=1}^{N} \gamma_j^k \varphi_j(\mathbf{x}_i)\right), \\ \sum_{j=1}^{N} \gamma_j^{k+1} \varphi_j(\mathbf{x}_i) - \frac{\tau}{2} \sum_{j=1}^{N} \lambda_j^{k+1} \varphi_j(\mathbf{x}_i) = \sum_{j=1}^{N} \gamma_j^k \varphi_j(\mathbf{x}_i) + \frac{\tau}{2} \sum_{j=1}^{N} \lambda_j^k \varphi_j(\mathbf{x}_i) - \tau (\gamma_u)_i{}^k, \\ \nu_u\left(\sum_{j=1}^{N} \alpha_j^{k+1} \varphi_j(\mathbf{x}_i)\right) + \frac{\sum_{j=1}^{N} \lambda_j^{k+1} \varphi_j(\mathbf{x}_i)}{2} - \frac{\sum_{j=1}^{N} \gamma_j^{k+1} \varphi_j(\mathbf{x}_i)}{2\delta} \\ \quad = \nu_u\left(\sum_{j=1}^{N} \alpha_j^k \varphi_j(\mathbf{x}_i)\right) - \frac{\sum_{j=1}^{N} \lambda_j^k \varphi_j(\mathbf{x}_i)}{2} + \frac{\sum_{j=1}^{N} \gamma_j^k \varphi_j(\mathbf{x}_i)}{2\delta}, \quad k = 0, 1, 2, \ldots, M-1. \end{cases} \tag{2.10}$$

On the other hand, for boundary conditions, we can write at boundary points ($i = N_I + 1, N_I + 2, \ldots, N_I + N_b$)

$$\sum_{j=1}^{N} \alpha_j^{k+1} \frac{\partial \varphi_j(\mathbf{x}_i)}{\partial \vec{\mathbf{n}}} = \sum_{j=1}^{N} \beta_j^{k+1} \frac{\partial \varphi_j(\mathbf{x}_i)}{\partial \vec{\mathbf{n}}} = \sum_{j=1}^{N} \gamma_j^{k+1} \frac{\partial \varphi_j(\mathbf{x}_i)}{\partial \vec{\mathbf{n}}} = \sum_{j=1}^{N} \lambda_j^{k+1} \frac{\partial \varphi_j(\mathbf{x}_i)}{\partial \vec{\mathbf{n}}} = 0, \quad k = 0, 1, 2, \ldots, M-1. \tag{2.11}$$

According to Eqs. (2.10) and (2.11), we obtain the following linear system of algebraic equations:

$$A\mathbf{y}^{k+1} = B\mathbf{y}^k + \mathbf{b}^k, \ k = 0, 1, 2, \ldots, M-1, \tag{2.12}$$

where A and B are coefficients matrices with size $4N \times 4N$ in the collocation points and $\mathbf{b}^k$ is a vector at the present time. Moreover, the vector $\mathbf{y}^{k+1}$ is unknown coefficients at level time $k+1-$th. After solving the linear system of algebraic equations (2.12), we can compute the unknown coefficients at the present level time i.e. $\mathbf{y}^{k+1}$. This procedure continues until, the time tends to the final time T. Then we replace the obtained unknown coefficients into Eq. (2.9) and the approximation solutions can be computed at each time over the entire domain Ω.

3. Efficient time integration as method of lines (MOL)

The implementation of the proposed methods such as GMLS technique can be performed with more efficiently if we apply an explicit time procedure to overcome time variable.

Here, an explicit time method based on Runge–Kutta approach will be used. To apply this procedure on Eq. (1.1), the following algorithm can be considered.

We first divide the time interval $[0, T]$ to M sub-intervals, in which $\Delta t = \frac{T}{M}$. An explicit fourth-order Runge–Kutta method for Eq. (1.1) can be implemented in the following procedure [50]

$$\begin{aligned} u^{k+1} &= u^k + \frac{1}{6}(m_1 + 2(m_2 + m_3) + m_4), \\ m_1 &= \Delta t\, F_u(t, u^k, \mu_u{}^k, n^k, \mu_n{}^k), \\ m_2 &= \Delta t\, F_u\left(t + \frac{\Delta t}{2}, u^k + \frac{m_1}{2}, \mu_u{}^k + \frac{m_1}{2}, n^k + \frac{mm_1}{2}, \mu_u{}^k + \frac{mm_1}{2}\right), \\ m_3 &= \Delta t\, F_u\left(t + \frac{\Delta t}{2}, u^k + \frac{m_2}{2}, \mu_u{}^k + \frac{m_2}{2}, n^k + \frac{mm_2}{2}, \mu_u{}^k + \frac{mm_2}{2}\right), \end{aligned}$$

$$
\begin{aligned}
m_4 &= \Delta t\, F_n(t+\Delta t, u^k+m_3, {\mu_u}^k+m_3, n^k+mm_3, {\mu_u}^k+mm_3),\\
n^{k+1} &= n^k+\frac{1}{6}(mm_1+2(mm_2+mm_3)+mm_4),\\
mm_1 &= \Delta t\, F_n(t, u^k, {\mu_u}^k, n^k, {\mu_n}^k),\\
mm_2 &= \Delta t\, F_n\left(t+\frac{\Delta t}{2}, u^k+\frac{m_1}{2}, {\mu_u}^k+\frac{m_1}{2}, n^k+\frac{mm_1}{2}, {\mu_u}^k+\frac{mm_1}{2}\right),\\
mm_3 &= \Delta t\, F_n\left(t+\frac{\Delta t}{2}, u^k+\frac{m_2}{2}, {\mu_u}^k+\frac{m_2}{2}, n^k+\frac{mm_2}{2}, {\mu_u}^k+\frac{mm_2}{2}\right),\\
mm_4 &= \Delta t\, F_n(t+\Delta t, u^k+m_3, {\mu_u}^k+m_3, n^k+mm_3, {\mu_u}^k+mm_3),\\
{\mu_u}^{k+1} &= f'(u^{k+1})-\varepsilon^2\Delta u^{k+1}+D_u\chi(u^{k+1}, n^{k+1}),\\
{\mu_n}^{k+1} &= D_n\chi(u^{k+1}, n^{k+1})+\frac{n^{k+1}}{\delta}, \quad k=0,1,\ldots,M-1.
\end{aligned}
\tag{3.1}
$$

For approximating the space variable, a local version of meshless technique such as GMLS approximation can be implemented. This scheme lets us to use more points for obtaining better results in simulations of the mathematical model studied in this manuscript. Note that, combining the above time integration using GMLS technique gives N systems of ordinary differential equations at each time step. Therefore, we never solve the nonlinear system at each time step.

Remark 3.1. It should be noted that, an explicit scheme will be applied at each time step. Therefore, the computational cost decreases in this case by increasing the collocation points in comparison with an implicit scheme.

4. Numerical simulations and validation of meshless methods

This part of the present numerical study involves the solution of four-species tumor growth time-dependent partial differential equation which gives some numerical experiments on the studied model to validate the meshless methods. For implementing discussed methods, some parameters are fixed. The radius of support domain is equal to $\delta = 4h$, where h is the distance between two neighbor points.

MQ radial basis function which will be applied in the following simulations is defined as follows [23,60]:

$$\phi(r) := \sqrt{r^2+c^2},$$

where c is shape parameter and it's value equals to $c = 0.05h$.

To compare between methods, we first examined on two simple examples. Since GMLS approximation is a localized method, we can use more collocation points on the region of the problem. Therefore, for finding suitable numerical solution of Eq. (1.1) with variable mobility i.e. $M_u = \overline{M}u^2$, GMLS procedure combined with an explicit Runge–Kutta method.

As is discussed in the previous sections, applying a semi-implicit time integration based on Crank–Nicolson procedure on Eq. (1.1) (when $M_u = \overline{M}$) gives the linear system of algebraic equations at each time-step. To solve this system at each time step, we can use the following command in MATLAB software as follows:

$$[\mathtt{L}, \mathtt{U}] = \mathtt{lu}(\mathtt{A},\mathtt{'vector'}),$$

where A is obtained with respect to Eq. (2.8) or (2.12).

Some numerical experiments are reported in the following subsections.

4.1. Evaluation of tumor-growth model with constant mobility in two-dimension

When in Eq. (1.1) the mobility function i.e. M_u is constant like [63], two presented meshless techniques are applied. The initial conditions are

$$
\begin{cases}
u(x,y,0) = \tanh\left(\dfrac{0.15-\sqrt{x^2+y^2}}{\sqrt{2}\varepsilon}\right),\\
n(x,y,0) = 1.
\end{cases}
$$

The region of the problem is a rectangle $[-1,1]\times[-1,1]$. This type of tumor-growth model describes a **single tumor** which was studied in [63]. The nonlinear free-energy density function i.e. $f(u)$ is chosen $f(u) = \frac{1}{4}(u^2-1)^2$. To show the evaluation of the solution at different times, required parameters such as $\epsilon = 0.02$, $P_0 = 300$, $\delta = 0.01$ have been fixed. The numerical solutions for both u and n are shown in Fig. 2 at $t = 0.0001, 0.008, 0.032$ and $t = 0.064$. This figure demonstrates increasing a tumor cell in period time. To reach these results via GMLS approximation, $\Delta t = 0.01h^2$, $h = 2/128$ are chosen.

Tumor-growth model also can describe **three tumors** which are located in the region of the problem. It also was studied in [63]. To show the evaluation of three tumors in time, the initial conditions for tumor cell and nutrient can be considered

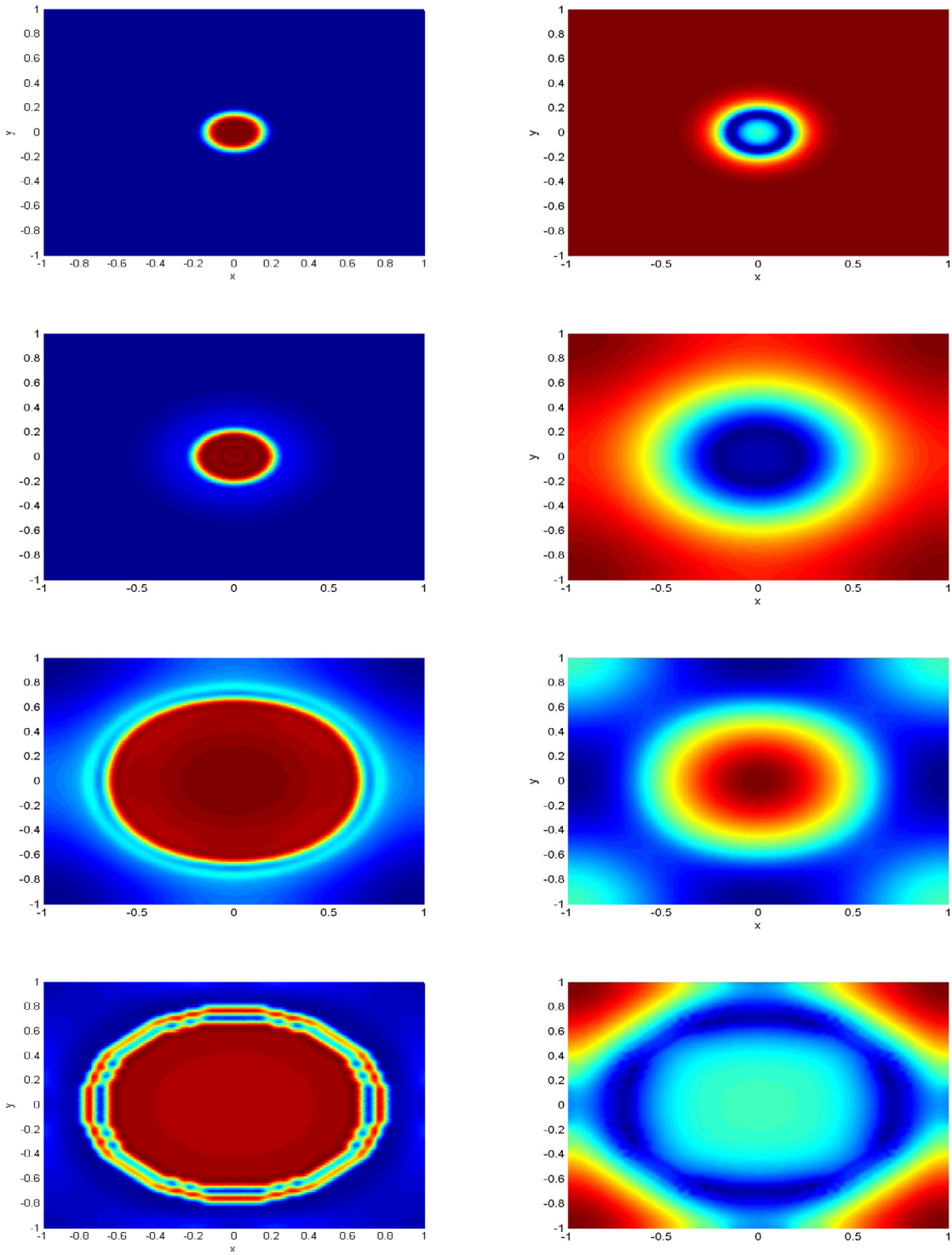

Fig. 2. The numerical solutions of both tumor cell (u) at left panel and nutrient (n) at right panel at different times for single tumor-growth.

Table 1
The required CPU time for constructing the coefficients matrix.

Method	CPU-time
GMLS	1.19 sec
RBFs	24.90

as [63]:

$$\begin{cases} u(x,y,0) = \tanh\left(\dfrac{0.15-\sqrt{(x-0.15)^2+(y-0.15)^2}}{\sqrt{2}\varepsilon}\right)+\tanh\left(\dfrac{0.15-\sqrt{(x-0.3)^2+(y-0.5)^2}}{\sqrt{2}\varepsilon}\right) \\ \quad +\tanh\left(\dfrac{0.15-\sqrt{(x+0.2)^2+(y+0.2)^2}}{\sqrt{2}\varepsilon}\right)+2, \\ n(x,y,0) = 1. \end{cases}$$

The nonlinear free-energy density function is defined as the previous case. All parameters are fixed with respect to the previous choices. The numerical solutions of tumor cell (u) and nutrient (n) are shown in Fig. 3 at $t = 0.0004, 0.008, 0.02$ and $t = 0.032$. As can be seen, the nutrient is consumed by tumor-growth in time. This phenomena also is observed in [63]. Table 1 shows the required CPU time for constructing the coefficients matrix in two meshless approaches for $h = 2/40$. As is expected, since the GMLS technique is a local approximation, the CPU time to construct coefficients matrix is less than the CPU time which requires for constructing coefficients matrix in RBFs method.

4.2. Evaluation of tumor-growth model with variable mobility, tumor growing in a moderately oxygenated region

For obtaining the approximation solution Eq. (1.1) with variable mobility, GMLS approximation is employed using more collocation points. This model was studied in [27]. Required parameters which are used here are as : $\overline{M} = 10$, $P_0 = 0.1$, $\overline{D} = 1$, $X_0 = 0.05$, $\delta = 0.01$, $\Gamma = 0.045$ and $\epsilon = 0.005$. The initial condition for tumor cell is taken to occupy the ellipsoidal domain [27]:

$$\left\{(x,y) \in \mathbb{R}^2 : \frac{(x-12.8)^2}{2.1}+\frac{(y-12.8)^2}{1.9} \le 1\right\}.$$

The region of the problem is rectangle [0.25.6] × [0, 25.6]. The numerical solutions for both tumor cell and nutrient are simulated at different times in Fig. 4. These simulations are obtained by choosing $\Delta t = 0.01h^2$ and $h = 25.6/128$. To demonstrate the effect of parameters, we obtained the numerical simulation of tumor cell and nutrient with $\delta = 0.01$ and $\delta = 0.1$. Also the value of X_0 is considered 0.5. The values of Γ, ϵ, $\overline{M}$, P_0 and $\overline{D}$ are chosen as above. As is observed in [27], the tumor immediately breaks apart and begins moving quickly toward the regions with higher nutrients when δ increases (see Fig. 5 at right panel).

4.3. Evaluation of tumor-growth model with variable mobility in three-dimensional

The tumor-growth model can be formulated in three-dimensional region as cubic [0, 25.6] × [0, 25.6] × [0, 25.6]. The initial condition for tumor cell is taken to occupy the ellipsoidal domain in three-dimensional region as follows:

$$\left\{(x,y,z) \in \mathbb{R}^3 : \frac{(x-12.8)^2}{2.1}+\frac{(y-12.8)^2}{1.9}+\frac{(z-12.8)^2}{1.7} \le 1\right\}.$$

Moreover, the initial condition for nutrient is considered $n(x,y,z,0) = 1$.

For simulating the tumor-growth model, we choose $\overline{M} = 10$, $P_0 = 0.1$, $\overline{D} = 1$, $X_0 = 0.4$, $\delta = 0.01$, $\epsilon = 0.01$ and $\Gamma = 0.25$. To obtain the evaluation of tumor cell at different times, we employ the GMLS approximation using explicit Runge–Kutta time integration. The collocation points are chosen 17576 and $\Delta t = 1 \times 10^{-2}$. Moreover, the radius of support domain is considered $\delta = 4$. Fig. 6 shows the tumor-growth at $t = 1, 5, 10$ and $t = 20$. It should be noted that, to draw three-dimensional tumor cell, we used the following commands in MATLAB software.

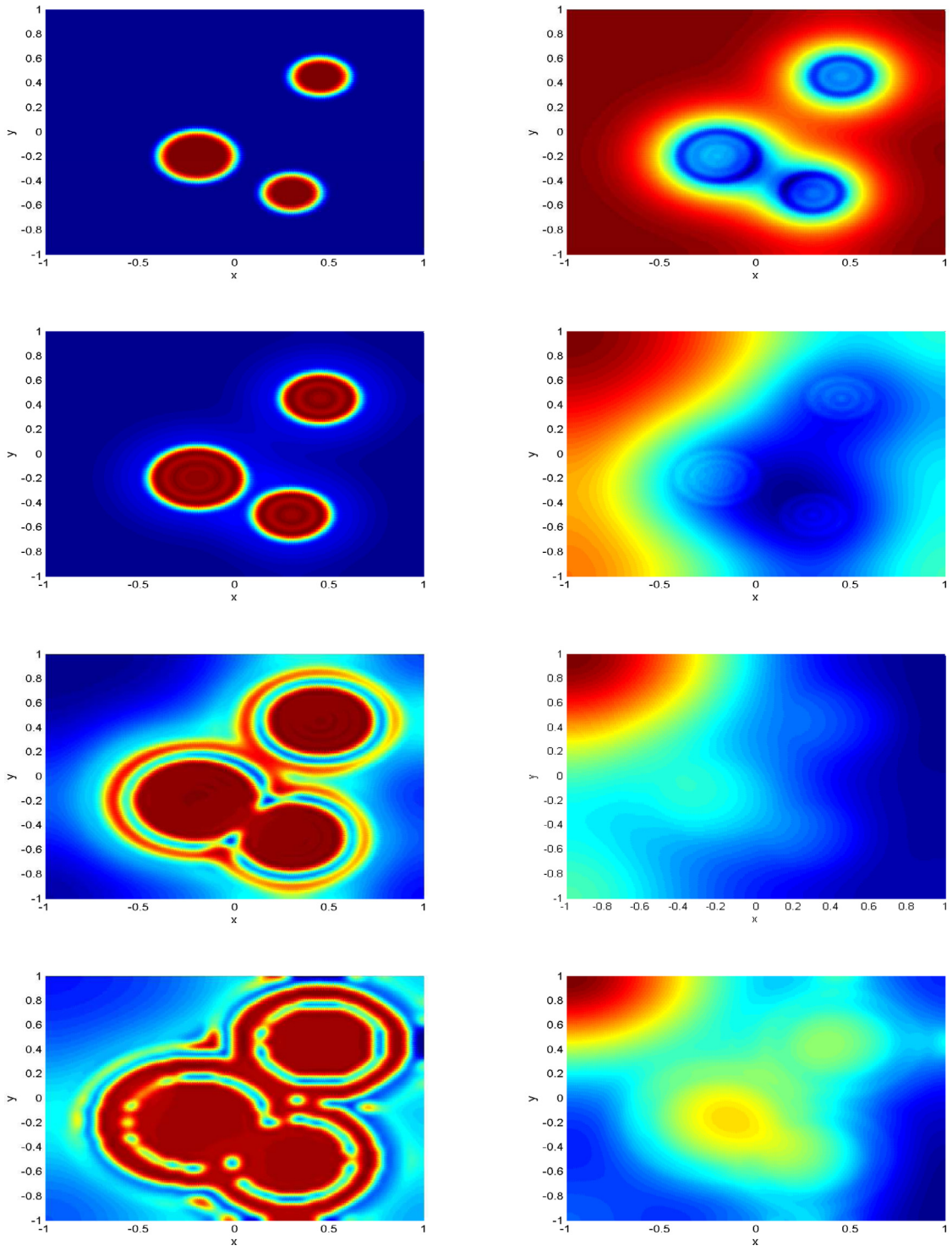

Fig. 3. The numerical solutions of both tumor cell (u) at left panel and nutrient (n) at right panel at different times for three tumors-growth.

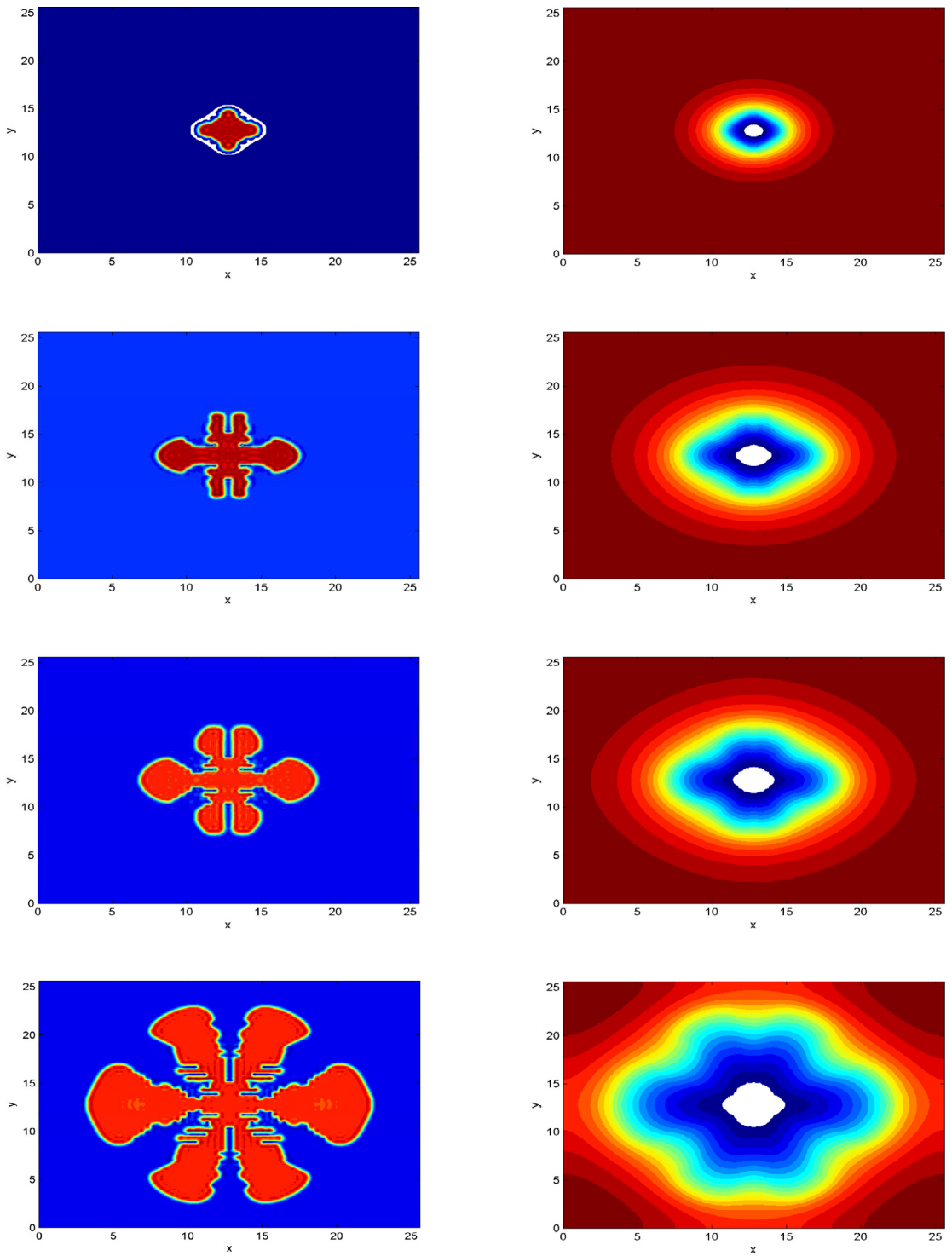

Fig. 4. The numerical solutions of both tumor cell (u) at left panel and nutrient (n) at right panel at different times for tumor growing in a moderately oxygenated region.

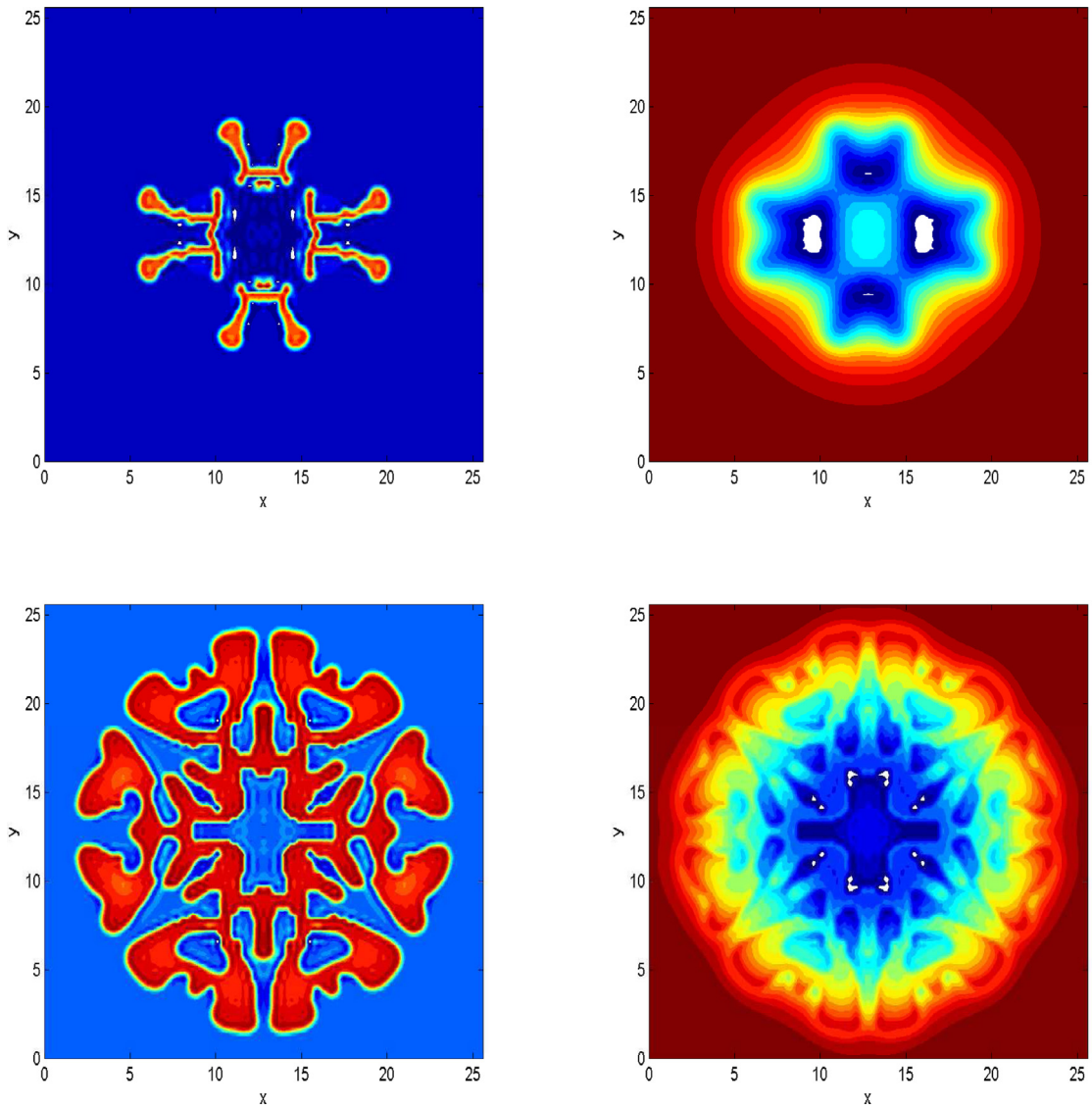

Fig. 5. The numerical solutions of both tumor cell (u) at left panel and nutrient (n) at right panel at different times for different values δ, $\delta = 0.01$ (first row) and $\delta = 0.1$ (second row).

```
[x,y,z] = meshgrid(a:h/4:b);
v = TriScatteredInterp(X(:,1),X(:,2),X(:,3),sparse(A)*U);
qvi =v(x,y,z);

figure, smooth3(qvi,'gaussian');
p1=patch(isosurface(x,y,z,qvi),'FaceColor','blue','EdgeColor','none');
p2 = patch(isocaps(x,y,z,qvi),'FaceColor','interp','EdgeColor','none');
isonormals(x,y,z,qvi,p1);
isocolors(x,y,z,qvi,p2);
isocaps(x,y,z,qvi);
view(3); axis vis3d tight
camlight; lighting phong
```

Note that, the vector `X(:,1:3)` denotes the collocation points in cubic domain and `sparse(A)` indicates the collocation matrix which is obtained from the collocation procedure when GMLS approximation is used.

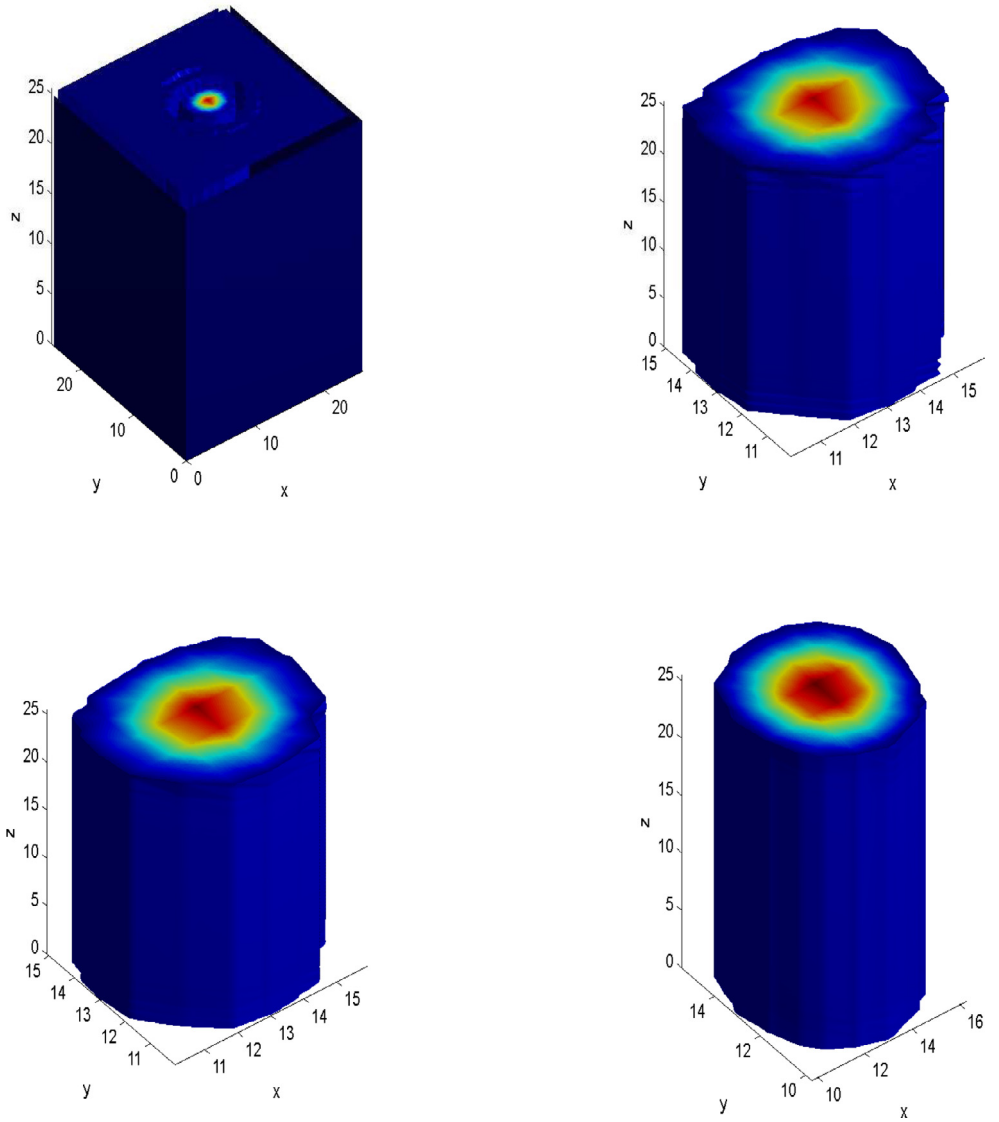

Fig. 6. The numerical solution of tumor cell (u) at different times in three-dimensional region.

5. Conclusion

In this paper, two numerical meshless methods planned for solving the four-species tumor-growth model in two and three-dimensional regions. As is mentioned, this model can be considered in two cases:

1. Tumor-growth model with constant mobility.
2. Tumor-growth model with variable mobility.
   Two meshless techniques are implemented based on the following approach.
   This approach is collocation technique as generalized moving least squares (GMLS) method and radial basis functions. GMLS technique approximates the derivatives of unknown function directly. It also uses a basis of polynomials for constructing of the approximation solution of the problem. This technique is implemented as localized approximation. RBFs method based on Kansa's approach approximates the derivatives of the unknown function according to the radial basis functions. It is also depends on shape parameter which can be influenced on the numerical solution. This technique is implemented as global approximation.
   The discretization of the time variable is performed by a semi-implicit finite difference method based on Crank–Nicolson scheme. To obtain the approximation solutions of the model with variable mobility efficiently, an explicit Runge–Kutta method is applied. With this scheme, at each time-step, the solutions can be computed without solving

nonlinear system of algebraic equations. Numerical simulations show the ability of the presented methods for solving the interesting models studied in the current paper.

Some important remarks can be noted as follows:

1. The implementation of meshless methods can be extended easily for different problems in high-dimensional cases.
2. They can compute the numerical solution of the problem with any choices of grid.
3. The use of local approximation gives better results in comparison with global method specially when the model contains variable mobility.
4. Choosing a suitable explicit time integration can be useful for finding good accuracy by increasing collocation points.

Acknowledgment

The authors are very grateful to reviewers for carefully reading this paper and for their comments and suggestions which have improved the paper.

References

[1] Araujo RP, McElwain DLS. A linear-elastic model of anisotropic tumour growth. Eur J Appl Math 2004;15:365–84.
[2] Araujo RP, McElwain DLS. A mixture theory for the genesis of residual stresses in growing tissues II: solutions to the biphasic equations for a multicell spheroid. SIAM J Appl Math 2005;66:447–67.
[3] Ambrosi D, Preziosi L. Cell adhesion mechanisms and stress relaxation in the mechanics of tumours. Biomech, Model Mechanobiol 2009;8(5):397–413.
[4] Atluri SN, Zhu T. A new meshless local Petrov-Galerkin (MLPG) approach in computational mechanics. Comput Mech 1998;22(2):117–27.
[5] Atluri SN, Shen SP. The meshless local Petrov-Galerkin (MLPG) method: a simple and less-costly alternative to the finite elementmethods. Comput Model Eng Sci 2002;3(1):11–51.
[6] Atluri SN. The Meshless Method (MLPG) for Domain and BIE Discretizations. Tech Science Press; 2004.
[7] Bartlett JM, Stirling D. A short history of the polymerase chain reaction. Methods Mol Cell Biol 2003;226:3–6.
[8] Breward CJW, Byrne HM, Lewis CE. The role of cell-cell interactions in a two phase model for avascular tumour growth. J Math Biol 2002;45:125–52.
[9] Bellomo N, Chaplain M, Angelis ED. Selected topics in cancer modeling: genesis, evolution, immune competition, and therapy. Springer, London; 2008.
[10] N Bellomo N, Li NK, Maini PK. On the foundations of cancer modelling: selected topics, speculations, and perspectives. Math Models Methods Appl Sci 2008;18(4):593–646.
[11] Boyer F, Minjeaud S. Numerical schemes for a three component Cahn-Hilliard model. Math Model Numer Anal 2011;45:697–738.
[12] Breward CJW, Byrne HM, Lewis CE. A multiphase model describing vascular tumour growth. Bull Math Biol 2003;65:609–40.
[13] Bowen RM. Theory of mixtures. In continuum physics, 3. Academic Press: New York; 1976.
[14] Byrne HM, Alarcon T, Owen MR, Webb SD, Maini PK. Modelling aspects of cancer dynamics: a review. Philos Trans R Soc Lond A 2006;364:1563–78.
[15] Chen YC, Byrne HM, King JR. The influence of growth-induced stress from the surrounding medium on the development of multicell spheroids. J Math Bio 2001;43:191–220.
[16] Chaplain MAJ, Graziano L, Preziosi L. Mathematical modelling of the loss of tissue compression responsiveness and its role in solid tumor development. Math Med Biol 2006;23(3):197–229.
[17] Cristini V, Li X, Lowengrub JS, Wise S. Nonlinear simulations of solid tumor growth using a mixture model: invasion and branching. J Math Biol 2009;58:723–63.
[18] Dehghan M, Shokri A. Numerical solution of the Klein-Gordon equation using radial basis functions. J Comput Appl Math 2009;230:400–10.
[19] Dehghan M, Shokri A. A numerical method for solution of the two dimensional Sine-Gordon equation using the radial basis functions. Math Comput Simul 2008;79:700–15.
[20] Dehghan M, Mirzaei D. Meshless local Petrov-Galerkin (MLPG) approximation to the two dimensional Sine-Gordon equation. J Comput Appl Math 2010;233:2737–54.
[21] Dehghan M, Salehi R. A meshless local Petrov-Galerkin method for the time-dependent Maxwell equations. J Comput Appl Math 2014;268:93–110.
[22] Du Q, Nicolaides RA. Numerical analysis of a continuum model of phase transition. SIAM J Numer Anal 1991;28:1310–22.
[23] Fasshauer GE. Meshfree approximation methods with MATLAB. Word Scientific Publishing Co. Pte. Ltd.; 2007.
[24] Fasano A, Bertuzzi A, Gandolfi A. Mathematical modelling of tumour growth and treatment. Complex Systems in Biomedicine 2006:71–108.
[25] Graziano L, Preziosi L. Mechanics in tumor growth. Modelling of Biological Materials 2007:263–321.
[26] Gomez H, Hughes TJR. Provably unconditionally stable, second-order time-accurate, mixed variational methods for phase-field models. J Comput Phys 2011;230:5310–27.
[27] Hawkins-Daarud A, van der Zee KG, Oden JT. Numerical simulation of a thermodynamically consistent four-species tumor growth mode. Int J Numer Meth Biomed Engng 2012;28:3–24.
[28] Hanahan D, Weinburg RA. The hallmarks of cancer. Cell 2000;100:57–70.
[29] Hu Z, Wise SM, Wang C, Lowengrub JS. Stable and efficient finite-difference nonlinear-multigrid schemes for the phase field crystal equation. J Comput Phys 2009;228:5323–39.
[30] Hu DA, Long SY, Liu KY, Li GY. A modified meshless local Petrov-Galerkin method to elasticity problems in computer modelling and simulation. Eng Anal Bound Elem 2006;30:399–404.
[31] Kansa EJ. Multiquadrics -a scattered data approximation scheme with applications to computational fluid-dynamics-i. Comput Math Appl 1990;19:127–45.
[32] Kansa EJ, Geiser J. Numerical solution to time-dependent 4d inviscid Burgers' equations. Eng Anal Bound Elem 2013;37:637–45.
[33] Kansa EJ, Aldredge RC, Ling L. Numerical simulation of two-dimensional combustion using mesh-free methods. Eng Anal Bound Elem 2009;33:940–50.
[34] Kansa EJ, Hon YC. Circumventing the ill-conditioning problem with multiquadric radial basis functions (RBFs) applications to elliptic partial differential equations. Comput Math Appl 2000;39:123–37.
[35] Kim J, Kang K, Lowengrub J. Conservative multigrid methods for Cahn-Hilliard fluids. J Comput Phys 2004;193:511–43.
[36] Lancaster P, Salkauskas K. Surfaces generated by moving least squares methods. Math Comput 1981;37:141–58.
[37] Lowengrub JS, Frieboes HB, Jin F, Chuang YL, Li X, Macklin P, et al. Nonlinear modelling of cancer: bridging the gap between cells and tumours. Nonlinearity 2010;23(1):1–9.
[38] Liu KY, Long SY, Li GY. A simple and less-costly meshless local Petrov-Galerkin (MLPG)method for the dynamic fracture problem. Eng Anal Bound Elem 2006;30:72–6.
[39] Liu GR, Gu YT. An introduction to meshfree methods and their programming. Springer, Netherlands; 2005.
[40] Mirzaei D. Error bounds for GMLS derivatives approximations of Sobolev functions. J Comput Appl Math 2016;294(1):93–101.
[41] Mirzaei D, Schaback R, Dehghan M. On generalized moving least squares and diffuse derivatives. IMA J Numer Anal 2012;32(3):983–1000.
[42] Mirzaei D, Schaback R. Direct meshless local Petrov-Galerkin (DMLPG) method: A generalized MLS approximation. Appl Num Math 2013;68:73–82.

[43] Mirzaei D. Analysis of moving least squares approximation revisited. J Comput Appl Math 2015;282:237–50.
[44] Oden JT, Hawkins A, Prudhomme S. General diffuse-interface theories and an approach to predictive tumor growth modeling. Math Models Methods Appl Sci 2010;20(3):477–517.
[45] Preziosi L. Cancer modelling and simulation. Boca Raton, Florida: Chapman and Hall/CRC; 2003.
[46] Please CP, Pettet GJ, McElwain DLS. A new approach to modelling the formation of necrotic regions in tumors. Appl Math Lett 1998;11:89–94.
[47] Please CP, Pettet GJ, McElwain DLS. Avascular tumour dynamics and necrosis. Math Models Methods Appl Sci 1999;9:569–79.
[48] Preziosi L, Farina A. On Darcys law for growing porous media. Int J Non Linear Mech 2001;37:485–91.
[49] Preziosi L, Tosin A. Multiphase modelling of tumor growth and extracellular matrix interaction: mathematical tools and applications. J Math Biol 2009;58(4):625–56.
[50] Quarteroni A, Sacco R, Saleri F. Numerical mathematics. Springer, New York; 2007.
[51] Rodriguez EK, Hoger A, McCulloch AD. Stress-dependent finite growth in soft elastic tissues. J Biomech 1994;27:455–67.
[52] Salehi R, Dehghan M. A generalized moving least square reproducing kernel method. J Comput Appl Math 2013;69:34–58.
[53] Shen J, Wang C, Wang X, Wise SM. Second-order convex splitting schemes for gradient flows with Ehrlich-Schwoebel type energy: applicaion to thin film epitaxy. SIAM J Numer Anal 2012;50:105–25.
[54] Skalak R, Zargaryan S, Jain RK, Netti PA, Hoger A. Compatibility and the genesis of residual stress by volumetric growth. J Math Biol 1996;34:889–914.
[55] Taleei A, Dehghan M. Direct meshless local Petrov-Galerkin method for elliptic interface problems with applications in electrostatic and elastostatic. Comput Methods Appl Mech Engrg 2014;278:479–98.
[56] Truesdell C, Toupin R. The classical field theories. Handbuch der Physik 1960;1:226–858.
[57] Wise SM, Lowengrub JS, Frieboes HB, Cristini V. Three-dimensional diffuse-interface simulation of multispecies tumor growth-i. model and numerical method. J Theor Biol 2008;253(3):523–43.
[58] Wise SM, Lowengrub JS, Cristini V. An adaptive multigrid algorithm for simulating solid tumor growth using mixture models. Math Comput Model 2011;53:1–20.
[59] Wodo O, Ganapathysubramanian B. Computationally efficient solution to the Cahn-Hilliard equation: Adaptive implicit time schemes, mesh sensitivity analysis and the 3d isoperimetric problem. J Comput Phys 2011;230:6037–60.
[60] Wendland H. Scattered data approximation. Cambridge Mongraph on Applied and Computational Mathematics, Cambridge University Press, New York; 2005.
[61] De Wit A, Dewel G, Borckmans P, Walgraef D. Three-dimensional dissipative structures in reaction-diffusion systems. Physica D 1992;61:289–96.
[62] Wodarz D, Komarova NL. Computational biology of cancer: lecture notes and mathematical modeling. World Scientific: Hackensak, NJ; 2005.
[63] Wu X, van Zwieten GJ, van der Zee KG. Stabilized second-order convex splitting schemes for Cahn-Hilliard models with application to diffuse-interface tumor-growth models. Int J Numer Meth Biomed Engng 2014;30:180–203.